ORGANOMETALLICS

Article

pubs.acs.org/Organometallics

Substituent Effects of the Backbone in α-Diimine Palladium Catalysts on Homo- and Copolymerization of Ethylene with Methyl Acrylate

Lihua Guo,[†,‡] Haiyang Gao,*[,†] Qirui Guan,[†] Haibin Hu,[†] Juean Deng,[†] Jun Liu,[†] Fengshou Liu,[†] and Qing Wu*[,†]

[†]DSAPM Laboratory, PCFM Laboratory, Institute of Polymer Science, School of Chemistry and Chemical Engineering, Sun Yat-Sen University, Guangzhou 510275, People's Republic of China

[‡]The Key Laboratory of Life-Organic Analysis, School of Chemistry and Chemical Engineering, Qufu Normal University, Qufu, Shandong 273165, People's Republic of China

Supporting Information

ABSTRACT: On the basis of different approaches for modifying α-diimine palladium catalysts, a series of methyl chloride palladium complexes with various α-diimine ligand backbones were synthesized and characterized. The corresponding cationic palladium complex chelating esters were further obtained by treatment of methyl chloride palladium complexes with methyl acrylate (MA). It was observed that decomposition of a cationic palladium complex chelating ester can occur to produce a new cationic palladium complex chelating two ligands and two counteranions, which provides a new pathway for deactivation of palladium catalysts and formation of palladium black by a fragmentation pattern with ester loss. These α-diimine palladium catalysts were employed in the homopolymerization of ethylene and copolymerization of ethylene and MA to evaluate substituent effects of the ligand backbone. A bulky camphyl α-diimine palladium catalyst was found to show better thermal stability and afford high-molecular-weight copolymer with higher incorporation of polar monomer. Longstanding living polymerization of ethylene was also achieved within 12 h using a bulky camphyl α-diimine palladium catalyst.

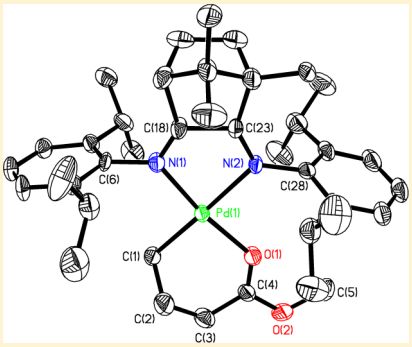

INTRODUCTION

Since Brookhart's initial reports, α-diimine palladium catalysts for olefin polymerization have received much attention because they can produce polyolefins with various types of branches and have good polar group tolerance.[1−19] One attractive feature of α-diimine palladium catalysts is their ability to precisely control polymer topology (linear, hyperbranched, and dendritic polyethylene) by varying ethylene pressure and polymerization temperature.[5−9] The reduced oxophilicity of the palladium center also gives the catalyst the ability to produce copolymers with a variety of polar-functionalized olefins.[2,3,9,15,19] Furthermore, a tandem polymerization strategy combining chain-walking polymerization using α-diimine palladium catalysts with controlled radical polymerizations such as atom transfer radical polymerization (ATRP)[20−24] or reversible addition−fragmentation chain transfer (RAFT) polymerization[25] has also been developed to synthesize functional copolymers.

Despite these striking features, α-diimine palladium catalysts are prone to deactivation under comparatively mild conditions via pathways that are still not completely clear. Palladium black in the polymerizing mixture is usually observed, strongly indicating the occurrence of catalyst decomposition during the polymerization process.[19] Brookhart and co-workers have shown that deactivation of α-diimine palladium catalysts can take place by C−H activation with alkyl groups on the α-diimine ligand to form palladacyclic intermediates.[26] Rotation of the ligand alkyl groups to the metal square plane is necessary in this process. Increasing the steric bulk of the ligand is therefore expected to make this process less favorable, thus enhancing the stability of the palladium catalyst. Numerous modifications to the α-diimine ligand have been reported, especially to the aniline moiety of the ligand.[9,12,27−30] For instance, cyclophane-based α-diimine palladium catalysts designed and synthesized by Guan[27] show better thermal stability for olefin polymerization and higher incorporation of methyl acrylate (MA) for copolymerization of ethylene and MA than the acyclic analogues.[28] The electronic effect of aniline moieties on the homo- and copolymerization of ethylene with MA has also been studied by Guan in detail.[29,30] In comparison with modification of the aniline moiety, modification of the backbone in α-diimine palladium catalysts has been rarely studied. To date, mainly three types of α-diimine ligand backbones (ArN═C(R)(R)C═NAr, R = H, Me, acenaphthene) have been used to synthesize palladium complexes.[9,19,31] Current literature has shown that changing the backbone substituent from hydrogen to a methyl group results in a significant increase in stability of the palladium catalyst and a decrease in chain transfer occurring via associative exchange from a palladium olefin hydride intermediate.[26] Increasing the bulk of the backbone substituent is thereby anticipated to

Received: May 7, 2012
Published: August 14, 2012

 © 2012 American Chemical Society dx.doi.org/10.1021/om300380b | *Organometallics* 2012, 31, 6054−6062

improve the stability and catalytic activity of the palladium catalyst.

Recently, we have addressed backbone effects of α-diimine nickel catalysts on the reactivity of ethylene polymerization and successfully explored a type of thermostable α-diimine nickel catalyst with a bulky camphyl backbone.[32] A bulky α-diimine nickel catalyst with a camphyl backbone is capable of polymerizing ethylene at 80 °C and also exhibits remarkable chain-walking ability. Introduction of camphyl on the ligand backbone can achieve polymerization performance similar to that of a cyclophane-based α-diimine ligand,[28] while camphyl α-diimine ligands are more conveniently accessible.[31,32] Inspired by the results of ethylene polymerization using a bulky camphyl α-diimine nickel catalyst,[32] we herein synthesize and characterize α-diimine palladium catalysts with various backbone structures such as camphyl, phenyl, 4-fluorophenyl, 4-methylphenyl, and methyl and investigate backbone substituent effects on the homo- and copolymerization of ethylene with MA in detail. A thermostable camphyl α-diimine palladium catalyst has been successfully discovered for living polymerization of ethylene, and it also is more tolerant to polar comonomers and affords copolymers with higher incorporation of MA. Additionally, we also present a new deactivation pathway of α-diimine palladium catalysts and the formation mechanism of palladium black.

RESULTS AND DISCUSSION

Synthesis of α-Diimine Palladium Complexes. The synthetic route for α-diimine palladium complexes is shown in Scheme 1. Four α-diimine ligands with phenyl and camphyl

Scheme 1. Synthetic Route of Cationic α-Diimine Palladium Complexes

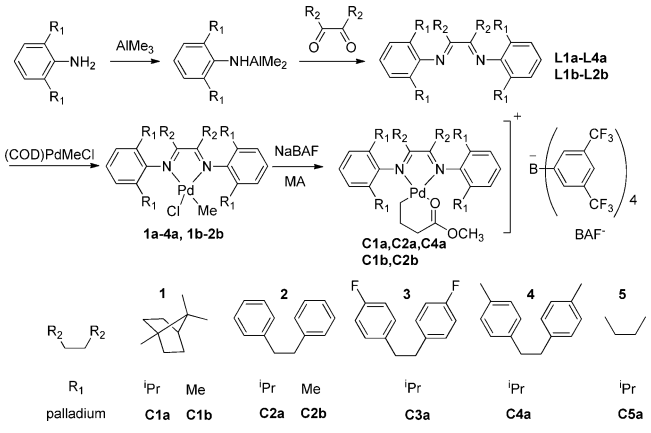

backbones were synthesized according to our previous report.[32] Two bulky α-diimine ligands with 4-fluorophenyl and 4-methylphenyl backbones (with two 2,6-diisopropylphenyl moieties) were also prepared to study the electronic effects of the ligand backbone. Complexation of α-diimine ligands and Pd(COD)MeCl (COD = 1,5-cyclooctadiene) afforded methyl chloride palladium complexes.[1−3] These methyl chloride palladium complexes were further treated with MA and sodium tetrakis(3,5-bis(trifluoromethyl)phenyl)borate (NaBAF) to yield the cationic palladium complexes [(α-diimine)Pd-$(CH_2)_3$C(O)OMe]$^+$BAF$^-$. However, an attempt to obtain the cationic palladium complex **C3a** with a 4-fluorophenyl backbone was unsuccessful under the same reaction conditions, which may result from the electron-withdrawing effect of the F group. All of the cationic palladium complexes were characterized by elemental analysis and NMR (see the Experimental Section). Brookhart previously reported that the five-membered chelate isomer was found in an α-diimine palladium complex with a methyl backbone (**C5a**), though the six-membered chelate is always predominant (>80%).[2,3] In contrast, ^{13}C NMR spectra of the obtained cationic palladium complexes confirm that only one six-membered chelate isomer exists in solution under the determined conditions. Only one resonance assigned to carbonyl (C═O) in the range 182.7−188.3 ppm was observed for each cationic palladium complex, suggesting the absence of the five-membered chelate isomer.

Crystal Structures. Single crystals of palladium complexes **2a**, **3a**, and **C1a** suitable for X-ray analysis were grown in hexane/CH_2Cl_2 solutions. ORTEP diagrams are given in Figures 1−3, respectively, along with selected bond lengths

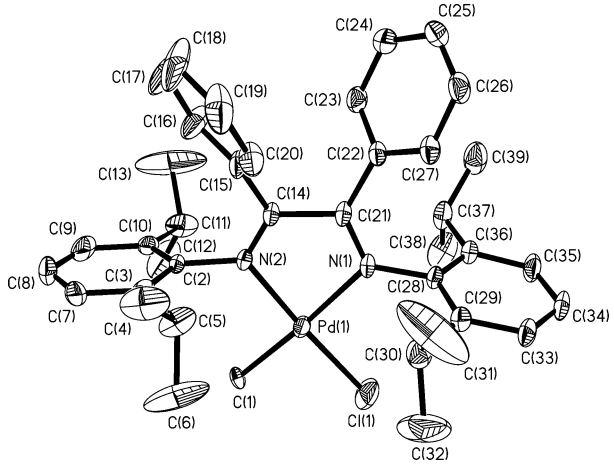

Figure 1. Molecular structure of complex **2a**. Hydrogen atoms are omitted for clarity. Selected bond distances (Å) and angles (deg): Pd(1)−C(1), 2.050(4); Pd(1)−N(2), 2.055(3); Pd(1)−N(1), 2.157(3); Pd(1)−Cl(1), 2.277(15); C(1)−Pd(1)−N(2), 98.53(15); C(1)−Pd(1)−N(1), 175.98(15); N(2)−Pd(1)−N(1), 77.45(13); C(1)−Pd(1)−Cl(1), 84.76(13); N(2)−Pd(1)−Cl(1), 176.60(10); N(1)−Pd(1)−Cl(1), 99.26(10); Pd(1)−N(2)−C(14), 116.0(3); Pd(1)−N(1)−C(21), 113.8(3).

and bond angles. The palladium complexes (α-diimine)-PdMeCl (**2a** and **3a**) feature a square-planar coordination of the central metal. The bond angles and distances in the palladium coordination plane are within the standard range for these types of complexes.[26] Two aniline moieties of **2a** and **3a** are nearly perpendicular to the five-membered coordination plane (dihedral angles of 89.6 and 89.4°), showing no obviously repulsive interactions between the aniline moiety and backbone substituents. The cationic palladium complex **C1a** also adopts a square-planar coordination geometry with the α-diimine ligand and 2,1-inserted MA.[33] The bond angles and distances in the palladium coordination plane are very close to the values for a cationic palladium complex with a methyl backbone reported by Ye.[24] It is significant to note that the *gem*-dimethyl substituents ($C(25)H_3$ and $C(26)H_3$) are oriented toward the axial position, indicating steric effects on the palladium metal center. In addition, the methyl ($C(27)H_3$) on the rigid camphyl lies out of one side, which may effectively suppress the potential rotation or fluctuation of the C_{Ar}−N bond, thus prohibiting C−H activation.[26,30]

dx.doi.org/10.1021/om300380b | Organometallics 2012, 31, 6054−6062

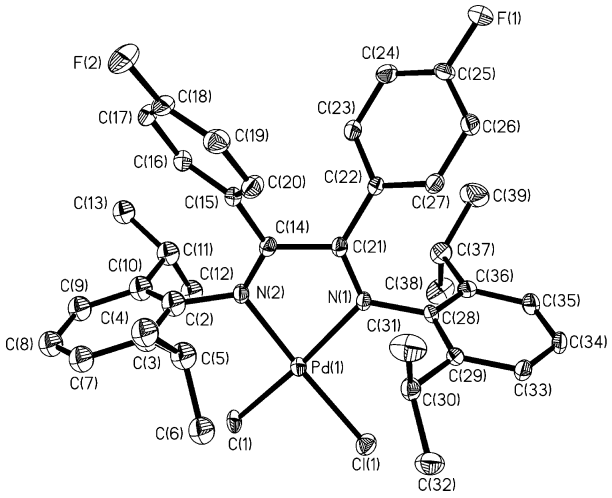

Figure 2. Molecular structure of complex **3a**. Hydrogen atoms are omitted for clarity. Selected bond distances (Å) and angles (deg): Pd(1)−C(1), 2.056(5); Pd(1)−N(2), 2.072(4); Pd(1)−N(1), 2.144(4); Pd(1)−Cl(1), 2.2802(13); C(1)−Pd(1)−N(2), 99.01(18); C(1)−Pd(1)−N(1), 175.60(18); N(2)−Pd(1)−N(1), 76.85(15); C(1)−Pd(1)−Cl(1), 86.38(15); N(2)−Pd(1)−Cl(1), 172.53(11); N(1)−Pd(1)−Cl(1), 97.88(11); Pd(1)−N(2)−C(2), 119.2(3); Pd(1)−N(1)−C(28), 121.7(3).

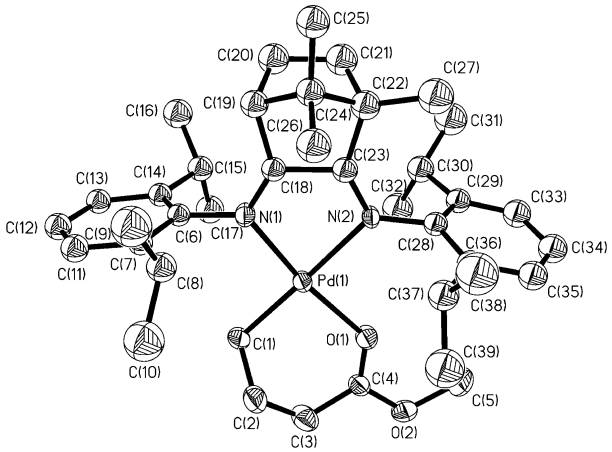

Figure 3. Molecular structure of complex **C1a**. The hydrogen and BAF^- anion are omitted for clarity. Selected bond distances (Å) and angles (deg): Pd(1)−C(1), 1.994(8); Pd(1)−O(1), 2.049(5); Pd(1)−N(1), 2.046(6); Pd(1)−N(2), 2.172(6); C(1)−Pd(1)−O(1), 90.6(3); C(1)−Pd(1)−N(1), 97.1(3); O(1)−Pd(1)−N(1), 172.1(2); C(1)−Pd(1)−N(2), 176.1(3); O(1)−Pd(1)−N(2), 92.2(2); N(1)−Pd(1)−N(2), 80.2(2).

Palladium Catalyst Stability. Generally, α-diimine palladium catalysts with ether auxiliary ligands for ethylene polymerization are prone to deactivation. On the basis of observation of low-temperature NMR spectra of α-diimine palladium with ether, Brookhart has previously presented a C−H activation mechanism.[19,26] Formed by the addition of MA, the stability of the cationic ester chelate palladium complex $[(\alpha\text{-diimine})Pd(CH_2)_3C(O)OMe]^+BAF^-$ can be improved through prohibition of C−H activation.[26] Nevertheless, decay of polymerization activity and precipitation of palladium black were often observed during ethylene polymerization using palladium catalysts with a chelating six-membered ester. This strongly suggests that a different deactivation pathway occurs by a reduction process from Pd(II) to Pd(0), though a detailed reduction process is still unclear.

It is interesting to note that the obtained palladium complex chelating esters $[(\alpha\text{-diimine})Pd(CH_2)_3C(O)OMe]^+BAF^-$ exhibit different stabilities. A clear trend is that palladium complexes bearing bulky ligands are more stable in solution. It is observed that the solution color of cationic palladium complex **C2b** slowly changed from orange to red and palladium black precipitated, suggesting decomposition of **C2b** and the appearance of a new palladium complex. A single crystal was obtained by careful treatment of the red solution and slow evaporation. Single-crystal X-ray diffraction data confirm that the new palladium complex $(\mathbf{L2b})_2Pd(BAF)_2$ is composed of two **L2b** chelate ligands, palladium metal, and two BAF counteranions (Figure 4). $(\mathbf{L2b})_2Pd(BAF)_2$ adopts a distorted

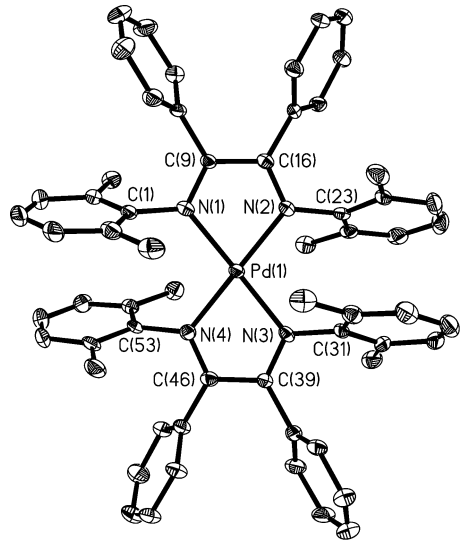

Figure 4. Molecular structure of complex $(\mathbf{L2b})_2Pd(BAF)_2$. The hydrogen, two BAF^- anions, and solvent molecules are omitted for clarity.

plane around the palladium atom, where the two α-diimine ligands act as bidentate N,N-chelators. Scheme 2 depicts the

Scheme 2. Deactivation Pathway of C2b and Formation of Palladium Black

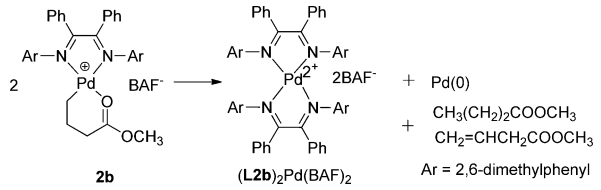

pathway of decomposition of **C2b** and formation of $(\mathbf{L2b})_2Pd(BAF)_2$ and palladium black. A molecule of **C2b** can abstract the ligand of another molecule to produce a molecule of $(\mathbf{L2b})_2Pd(BAF)_2$ and a molecule of palladium black. GC-MS analysis of the organic fraction confirmed the existence of ester compounds, including methyl butyrate and methyl but-3-enoate, further supporting this deactivation pathway. This is the first direct identification of a detailed reduction pathway of a α-diimine palladium(II) catalyst to palladium black. This new deactivation pathway provides access to a better understanding of how to optimize and design thermostable α-diimine

dx.doi.org/10.1021/om300380b | Organometallics 2012, 31, 6054−6062

palladium catalysts. Therefore, increasing the steric hindrance not only can retard chain transfer by associative exchange but also can inhibit deactivation of α-diimine palladium catalysts by a fragmentation pattern with ester loss.

Ethylene Polymerization. All of the palladium catalysts were screened for ethylene polymerization to evaluate substituent effects at 35 °C, and the detailed polymerization results are summarized in Table 1 (entries 1−6). Ethylene

Table 1. Ethylene Polymerizations with Different α-Diimine Palladium Catalysts[a]

entry	cat.	T_p (°C)	TOF[b]	M_n[c]	M_w[c]	PDI[c]	BD[d]
1	**C1a**	35	2132	28.8	44.6	1.55	86
2	**C2a**	35	458	25.9	42.2	1.63	85
3	**3a**[e]	35	185	22.4	33.8	1.51	84
4	**C4a**	35	491	41.8	69.8	1.67	93
5	**C1b**	35	467	9.5	14.3	1.50	107
6	**C2b**	35	442	3.1	4.7	1.51	104
7	**C1a**	5	193	9.5	10.9	1.15	89
8[f]	**C1a**	5	208	10.9	11.6	1.06	85
9	**C1a**	20	958	26.8	39.4	1.47	86
10	**C1a**	50	872	19.3	30.1	1.57	89
11	**C1a**	70	638	15.1	26.7	1.79	91
12	**C2a**	70	0				
13	**C5a**	70	trace	[g]			

[a]Reaction conditions: 10 μmol of catalyst, ethylene pressure 400 psi, solvent 50 mL of toluene, reaction time 2 h. Polymerizations were quenched by triethylsilane. [b]Turnover frequency, which is calculated as the moles of monomer per mole of palladium per hour, in units of h^{-1}. [c]Determined by GPC calibration using polystyrene standards. [d]Branching density, branches per 1000 carbons, determined by ^1H NMR. [e]In situ activated by 2 equiv of NaBAF. [f]The solvent is chlorobenzene. [g]Not determined.

polymerizations were directly initiated by addition of ethylene of 400 psi and reaction for 2 h. Because the cationic palladium catalyst **C3a** could not be obtained, ethylene polymerizations were carried out by an in situ activation of **3a** with 2 equiv of NaBAF.

The two new palladium catalysts **C1a** with camphyl and **C2a** with phenyl were first employed in the homopolymerization of ethylene to evaluate the substituent effects of the ligand backbone. A comparison of entries 1 and 2 in Table 1 demonstrates that **C1a** with a camphyl backbone shows a higher turnover frequency (TOF), up to 2132 h^{-1}, and yielded a higher molecular weight of polyethylene (28.8 kg/mol) than did **C2a** with a phenyl backbone. When phenyl groups were substituted on the backbone of the α-diimine instead of a camphyl group, a massive drop of 79% in the TOF was observed. This same effect of the backbone framework of α-diimine palladium catalyst as for a nickel catalyst may be explained as the electron-withdrawing and conjugate effect of phenyl.[32]

It was reported that a bulky aniline moiety is required for α-diimine palladium catalysts to achieve high TOF and high-molecular-weight polymer.[1,2] An attempt to optimize the steric effects of α-diimine ligand framework by the increasing steric bulk of the backbone and reducing the steric hindrance of aniline moiety is impractical. The steric bulk of the aniline moiety is more important than the steric bulk of the backbone. Decreasing the steric hindrance of the aniline moiety with a fixed backbone results in a drop in TOF and molecular weight of the PE (**C1a** vs **C1b**, **C2a** vs **C2b**). For example, camphyl **C1a** with 2,6-diisopropyl groups on the aniline moiety afforded high-molecular-weight polymer (44.6 kg/mol) with a TOF of 2132 h^{-1} (entry 1), while camphyl **C1b** with 2,6-dimethyl groups afforded low-molecular-weight products (14.6 kg/mol) with a TOF of 467 h^{-1} (entry 5). In addition, reducing the steric hindrance of the aniline moiety by substituting *o*-methyl groups for *o*-isopropyl groups also results in a reduced polymerization rate. **C1a** showed a rather stable ethylene consumption flow, as monitored by an ethylene flow rate meter over a period of 6 h, while **C2a** exhibited slightly reduced ethylene consumption. It was found that the ethylene consumption flow with **C2b** decreased constantly during the polymerization process over 6 h, and only slight consumption of ethylene was observed after 6 h. Simultaneously, a large quantity of palladium black precipitated, suggesting deactivation of palladium complex **C2b**. This observation can be well explained by the decomposition pathway of **C2b** presented in Scheme 2. On prolonging the reaction time, two molecules of **C2b** gradually decompose to $(\mathbf{L2b})_2Pd(BAF)_2$ and a molecule of palladium black. $(\mathbf{L2b})_2Pd(BAF)_2$ is inactive for ethylene coordination polymerization because of the absence of a Pd−C bond. Thus, reducing the palladium active center in the catalytic system leads to reduced ethylene consumption. Also note that decomposition of palladium complex **C2b** was accelerated in the presence of ethylene in comparison to that for a **C2b** solution in CH_2Cl_2, which may be attributed to the fact that ethylene makes ester chelate opening more favorable.[3]

Considering the easy modification of the backbone phenyl, we further designed and synthesized two other palladium analogues, **3a** and **C4a**, and studied the electronic effects of the para substituent on the backbone phenyl. A comparison of entries 2 and 3 demonstrates that introduction of F on the para position of the aryl leads to a decrease in TOF and molecular weight of the polyethylene. When methyl is used instead of F, increasing the TOF and molecular weight of the polyethylene can be observed (entries 2 and 4). Introduction of an electron-donating group on the α-diimine ligand backbone leads to the formation of high-molecular-weight polyethylene with an enhanced activity, which is in accord with that of a para substituent on the aniline moiety.[29] In addition, a catalyst with an electron-donating methyl group, **C4a**, was found to afford polymer with high branching density, which is in contrast with the electronic effect of the aniline moiety.[29] This result shows that there are different electronic effects of the aniline moiety and backbone on the chain-walking ability of the palladium center.

It is known that the Brookhart-type palladium catalyst **C5a** has poor thermal stability, and the reported ethylene polymerizations were generally carried out below 35 °C.[19,26,34,35] Herein, catalyst **C5a** only afforded a trace of polymer at 70 °C (entry 13), while catalyst **C2a** afforded no polymer (entry 12). Catalyst **C1a**, containing a camphyl backbone, showed higher thermal stability for ethylene polymerization than its α-diimine palladium analogues. Table 1 also gives the results of ethylene polymerizations with **C1a** in the temperature range 5−70 °C (entries 1 and 7−11). The observed basic trend is that the TOF of **C1a** reaches a maximum value at 35 °C and then decreases with elevated temperature. Even at 70 °C, a good TOF of 638 h^{-1} and a molecular weight of 15.1 kg/mol can be achieved. We attribute the enhanced thermal stability of catalyst **C1a** to its rigid and bulky bicyclic-substituted backbone, which can prohibit C−H activation by free C_{Ar}−N bond rotation or

dx.doi.org/10.1021/om300380b | Organometallics 2012, 31, 6054−6062

fluctuation[32] and deactivation by the fragmentation pattern presented in Scheme 2.

Note that molecular weight distributions (PDIs) of the polymers become narrow with decreasing temperature. PDI values of 1.15 can be achieved at 5 °C using **C1a** in toluene (entry 7). When chlorobenzene was used instead of toluene, a narrower polydispersity of 1.06 was observed (entry 8). Therefore, living polymerizations of ethylene were performed at 5 °C with a pressure of 400 psi in chlorobenzene. Polymerizations were quenched with Et_3SiH prior to polymer isolation to avoid the occurrence of chain coupling. Figure 5b shows monomodal GPC traces of the polymers obtained using **C1a** at different polymerization times, which shift to the higher molecular weight region with longer polymerization times. Plots of number-average molecular weight (M_n) and M_w/M_n (PDI) as a function of polymerization time (Figure 5a) also illustrate that M_n grows linearly with the polymerization time, and the PDI values are below 1.10. PE with an M_n value of ~34 is formed after 12 h using **C1a**, and its molecular weight is still precisely controlled (PDI = 1.09). No obvious palladium black was found in an aliquot sample of 12 h polymerization. This result supports the notion that the palladium catalyst is stable and long-lived under the adopted conditions. Therefore, ethylene polymerizations using **C1a** proceed in a living manner over 12 h. To the best of our knowledge, camphyl palladium catalyst **C1a** is one of the rare late-transition-metal catalytic systems for living polymerization of ethylene.[36−40] Living polymerization of ethylene using camphyl palladium catalyst **C1a** provides a viable access to the precise synthesis of monodisperse PE and corresponding block copolymers.

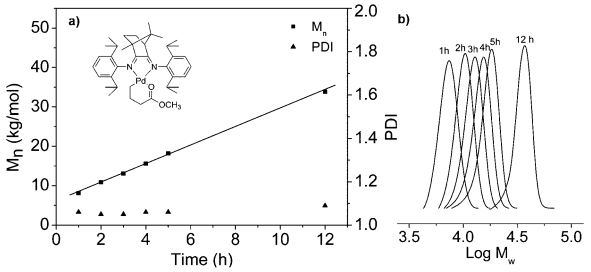

Figure 5. (a) Plots of M_n (■) and M_w/M_n (PDI) (▲) as a function of polymerization time using **C1a** at 5 °C (polymerization conditions: 400 psi, 10 μmol of Pd, 50 mL of chlorobenzene, reactions quenched by triethylsilane). (b) GPC traces at different times.

Copolymerization of Ethylene with MA. One striking feature of palladium catalysts is their good copolymerization ability for ethylene with a polar monomer. The electronic effects of substituents of the aniline moiety on the copolymerization of ethylene with MA were previously reported by Guan.[29,30] We herein investigated the effects of backbone substituents on the copolymerization of ethylene with MA. MA incorporation in the copolymer can be clearly identified by ^{1}H NMR of ethylene−MA copolymer (E-MA) (Figure 6) and can be calculated by eq 1. Results in Table 2 show that the backbone substituent has an important influence on the incorporation of MA. A clear trend is that a backbone containing an aryl group leads to a great drop in TOF and incorporation of MA. **C2a** and **3a** hardly show copolymerization TOF (entries 15 and 16), while **C4a** with a 4-methylphenyl backbone can afford low-molecular-weight copolymer with low incorporation of MA (entry 17). This

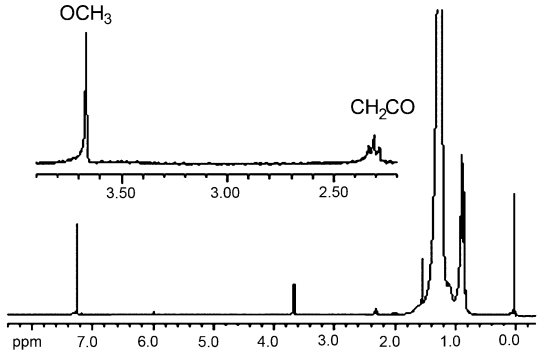

Figure 6. ^{1}H NMR spectrum of E-MA copolymer catalyzed by **C1a**.

Table 2. Copolymerization of Ethylene and MA with α-Diimine Palladium Catalysts[a]

entry	cat.	TOF[b]	MA incorp (mol %)[c]	M_n[d]	M_w[d]	PDI[d]	BD[e]
14	**C1a**	11	1.2	12000	19100	1.59	84
15	**C2a**	0					
16	**3a**[f]	0					
17	**C4a**	15	0.32	5600	8700	1.57	89
18	**C1b**	13	0.50	1500	3300	2.20	95
19	**C2b**	trace	0.30	2000	4200	2.09	93
20	**C5a**	66	0.52	12100	19000	1.57	99

[a]Reaction conditions: 30 μmol of catalyst, reaction temperature 35 °C, monomer concentration 0.5 M, ethylene pressure 15 psi, solvent CH_2Cl_2, total volume 100 mL, reaction time 36 h. Polymerizations were quenched by triethylsilane. [b]Turnover frequency, in units of h^{-1}. Because of the low yield and incorporation of MA, the TOF of MA is omitted. [c]Determined by ^{1}H NMR. [d]Determined by GPC calibration using polystyrene standards. [e]Branching density, branches per 1000 carbons, determined by ^{1}H NMR. [f]In situ activated by 2 equiv of NaBAF.

observation is in contrast to the electronic effects of substituents of the aniline moiety reported by Guan,[29] also suggesting different electronic influences on the incorporation of MA between the backbone and aniline moiety. It is interesting to note that the camphyl palladium catalyst shows the highest incorporation of MA among these catalysts (1.2 mol %) (entry 14), though the Brookhart-type palladium catalyst **C5a** exhibits the highest TOF (entry 20). The copolymers obtained by **C1a** and **C5a** also have nearly the same molecular weights. Presumably, binding of the electron-deficient olefin (MA) relative to ethylene is increased by enhancement of the steric bulk of the backbone substituents. The unique *gem*-dimethyl structure of the camphyl backbone can reduce the rate of comonomer exchange, thus enhancing the incorporation of olefins.[28] As for ethylene homopolymerization, reducing the steric bulk of the aniline moiety of the palladium catalyst results in a drop in molecular weight of the copolymerization product. Camphyl palladium complex **C1b** with 2,6-dimethylphenyl only can afford a copolymer with an M_n value of 1500. Therefore, the steric bulk of the aniline moiety has more significant influence on copolymerization than that of the backbone.

$$\mathrm{BD} = 1000 \times \frac{2(I_{\mathrm{CH_3}})}{3(I_{\mathrm{CH_2+CH}} + I_{\mathrm{CH_3}})} \quad (1)$$

dx.doi.org/10.1021/om300380b | *Organometallics* 2012, 31, 6054−6062

CONCLUSIONS

A series of $Pd^{II}(\alpha$-diimine)MeCl complexes and cationic $[Pd^{II}(\alpha$-diimine)$(CH_2)_3C(O)OMe]^+BAF^-$ complexes with various backbone frameworks were synthesized and characterized. A new pathway of decomposition of cationic palladium complexes and formation mechanism of palladium black by a fragmentation pattern with ester loss was presented and confirmed. Overall, the substituent effects of the backbone in α-diimine palladium catalysts are usually different from the substituent effects of the aniline moiety and are less significant for homopolymerization of ethylene and copolymerization of ethylene with MA. The camphyl α-diimine palladium catalyst was found to show better thermal stability for ethylene homopolymerization and afford high-molecular-weight E-MA copolymer with high incorporation of polar monomer, though the Brookhart-type α-diimine palladium catalyst with a methyl backbone exhibited the highest TOFs for copolymerization of ethylene with MA. This provides a different approach for enhancing the stability and tolerance to polar comonomer of α-diimine palladium, which complements the previous strategy of modifying the aniline moiety of α-diimine palladium. By optimizing the reaction conditions, longstanding living polymerization of ethylene can be also achieved using a bulky camphyl α-diimine palladium catalyst.

EXPERIMENTAL SECTION

General Considerations. All manipulations involving air- and moisture-sensitive compounds were carried out under an atmosphere of dried and purified nitrogen with standard vacuum-line, Schlenk, or glovebox techniques.

Materials. 2,6-Dimethylaniline and 2,6-diisopropylaniline were purchased from Aldrich Chemical and were distilled under reduced pressure before being used. TMA (1 M, hexane) was purchased from Aldrich Chemical. Benzil, 4,4′-dimethylbenzil, 4,4′-difluorobenzil, and L-camphorquinone were purchased from Alfa Aesar Chemical and used as received. Toluene, hexane, and diethyl ether were refluxed over metallic sodium for 24 h before being used. Dichloromethane and chlorobenzene were dried over phosphorus pentoxide for 8 h and distilled under a nitrogen atmosphere. Methyl acrylate was dried over CaH_2 prior to use in polymerization. $CDCl_3$ was dried over CaH_2 prior to use in NMR for palladium complexes. Et_3SiH (98%) was purchased from Alfa Aesar and used as received. (COD)PdMeCl[10] and the complexes $[(ArN{=}C(Me)C(Me){=}NAr)Pd^{II}(CH_2)_3C(O)OMe]^+BAF^-$ (**C5a**) were prepared according to literature methods.[1−3]

Characterization. Elemental analyses were performed with a Vario EL series elemental analyzer from Elementar. The NMR data of ligands and polymer samples were obtained on a Varian Mercury-Plus 300 MHz spectrometer at ambient temperature, using $CDCl_3$ as solvent, and referenced versus TMS as standard. The molecular weight and the molecular weight distribution (PDI) of the polyethylenes were determined on a Waters Breeze instrument at 40 °C, and THF was employed as the eluent at a flow rate of 1.0 mL/min. The GC-MS data were recorded with a Finnigan Voyager GC-8000 TOP series GC-MS system with a DB-5MS GC column.

Crystal Structure Determination. The X-ray diffraction data of single crystals were obtained with the $\omega-2\theta$ scan mode on a Bruker SMART 1000 CCD diffractometer with graphite-monochromated Mo Kα radiation (λ = 0.710 73). The structure was solved using direct methods, and further refinement with full-matrix least-squares on F^2 was obtained with the SHELXTL program package. All non-hydrogen atoms were refined anisotropically. Hydrogen atoms were introduced in calculated positions with the displacement factors of the host carbon atoms.

Ethylene Polymerization. A mechanically stirred 100 mL Parr reactor was heated to 150 °C for 2 h under vacuum and then cooled to room temperature. The autoclave was pressurized to 100 psi of ethylene and vented three times. The autoclave was then charged with 48 mL of solvent (toluene or chlorobenzene) under 200 psi of ethylene at the initialization temperature. The system was maintained by continuous stirring for 5 min, and then 2 mL of a solution of the palladium catalyst (**3a** was activated by 2 equiv of NaBAF) was charged into the autoclave under 200 psi of ethylene. The ethylene pressure was raised to the specified value (400 psi), and the reaction was carried out for a certain time. Polymerization was terminated by addition of 1.0 mL of triethylsilane after releasing the ethylene pressure. The solvents were removed on a rotary evaporator. When chlorobenzene was used as the polymerization medium, any residual chlorobenzene was removed under vacuum overnight. The obtained polymer was dissolved in hexane and filtered through a plug of silica gel to remove palladium black before precipitating in methanol. The resulting precipitated polymers were collected and treated by filtering, washing with methanol several times, and drying under vacuum at 40 °C to a constant weight.

Copolymerization of Ethylene and MA. In a typical procedure, a 250 mL round-bottom Schlenk flask with a stirring bar was heated for 3 h to 150 °C under vacuum and then cooled to room temperature. The flask was pressurized to 15 psi of ethylene and vented three times. The appropriate CH_2Cl_2 solvent and MA were introduced into the glass reactor under an ethylene atmosphere at 35 °C. The system was maintained by continuous stirring for 10 min, and then a 10 mL solution of the palladium catalyst (30 μmol) (**3a** was activated by 2 equiv of NaBAF) in CH_2Cl_2 was syringed into the well-stirred solution and the total reaction volume was kept at 100 mL. The ethylene pressure was kept at a constant value of 15 psi by continuous feeding of gaseous ethylene throughout the reaction. The polymerizations were terminated by the addition of a large amount of methanol after continuous stirring for 36 h. Then the methanol was decanted off, and the sticky polymer was redissolved in petroleum ether. The polymer solution was filtered through alumina and silica to remove catalyst residues. The resulting precipitated polymers were collected and treated by concentration and drying under vacuum at 40 °C to a constant weight. The MA incorporation (mol %) was calculated from ^1H NMR analysis, as was done before in previous studies of MA copolymers.[2]

Synthesis of Ligands. α-Diimine ligands were prepared according to our previously reported method[32] and fully characterized by NMR and elemental analysis.

*Synthesis of 2,6-(^{i}Pr)$_2$C$_6$H$_3$N=C(camphyl)C(camphyl)=N-2,6-(^{i}Pr)$_2$C$_6$H$_3$ (**L1a**).* Under a nitrogen atmosphere, 2,6-diisopropylphenylaniline (2.124 g, 12 mmol) in toluene (20 mL) solution was injected into a Schlenk flask, trimethylaluminum (12 mL, 1.0 M in hexane) was added slowly by a syringe at room temperature, and then the reaction mixture was heated to reflux for 2 h. After the solution was cooled to ambient temperature, L-camphorquinone (0.83 g, 5 mmol) was added. The mixture was stirred for another 6 h at reflux temperature. After the solution was cooled to 0 °C, the reaction mixture was carefully hydrolyzed with 5% aqueous NaOH solution. The desired product was obtained by extraction with ethyl acetate and evaporation. The crude product was further purified by column chromatography on silica gel using petroleum ether/ethyl acetate as eluent and was crystallized from ethanol as yellow crystals in 38.0% yield. A mixture of two geometrical isomers was determined by NMR, which is consistent with our previous report.[32] ^1H NMR (300 MHz, $CDCl_3$; δ (ppm) (an isomer ratio of 1.8:1])): major isomer, 7.06−6.81 (m, 6H, Ar-*H*), 2.88 (m, 4H, C*H*$(CH_3)_2$), 2.36 (m, 1H, tertiary hydrogen at camphyl), 1.86 (m, 4H, CH_2 at camphyl), 1.24 (d, 24H, CH(CH_3)$_2$), 0.96 (s, 6H, CH_3 at camphyl), 0.77 (s, 3H, CH_3 at camphyl); minor isomer, 7.06−6.81 (m, 6H, Ar-*H*), 2.69 (m, 4H, C*H*$(CH_3)_2$), 2.36 (m, 1H, tertiary hydrogen at camphyl), 1.86 (m, 4H, CH_2 at camphyl), 1.12 (d, 24H, CH(CH_3)$_2$), 0.94 (s, 6H, CH_3 at camphyl), 0.77 (s, 3H, CH_3 at camphyl). ^{13}C NMR (75 MHz, $CDCl_3$; δ (ppm)): major isomer, 168.57 (*C*=N), 144.89 (*C*-N), 136.10 (C_{Ar}-^{i}Pr), 122.53, 121.78, 55.92, 50.68, 45.43, 32.27, 28.41, 24.64, 22.44, 17.97, 11.30; minor isomer, 168.57 (*C*=N), 144.89 (*C*-N), 134.71 (C_{Ar}-^{i}Pr), 123.42, 121.46, 55.92, 50.68, 45.43, 32.27, 28.70, 24.73, 22.96, 17.97, 11.30.

dx.doi.org/10.1021/om300380b | *Organometallics* 2012, 31, 6054−6062

Anal. Calcd for $C_{34}H_{48}N_2$: C, 84.24; H, 9.98; N, 5.78. Found: C, 84.13; H, 9.87; N, 5.69.

*Synthesis of 2,6-(Me)$_2$C$_6$H$_3$N=C(camphyl)C(camphyl)=N-2,6-(Me)$_2$C$_6$H$_3$ (**L1b**).* Following the above procedure, **L1b** was isolated as yellow crystals in 84.7% yield. ^{1}H NMR (300 MHz, $CDCl_3$; δ (ppm) (an isomer ratio of 1.2:1)): major isomer, 6.86−6.70 (m, 6H, Ar-*H*), 2.07 (s, 12H, C_{Ar}-CH_3), 1.79 (m, 4H, CH_2 at camphyl), 1.39 (m, 1H, tertiary hydrogen at camphyl), 1.26 (s, 3H, CH_3 at camphyl), 1.07 (s, 6H, CH_3 at camphyl); minor isomer, 6.86−6.70 (m, 6H, Ar-*H*), 2.04 (s, 12H, C_{Ar}-CH_3), 1.86 (m, 4H, CH_2 at camphyl), 1.42 (m, 1H, tertiary hydrogen at camphyl), 1.26 (s, 3H, CH_3 at camphyl), 0.93 (s, 6H, CH_3 at camphyl). ^{13}C NMR (75 MHz, $CDCl_3$; δ (ppm)): major isomer, 170.87 (*C*=N), 149.37 (*C*-N), 127.53 (C_{Ar}-CH_3), 123.96, 122.71, 55.30, 51.18, 45.46, 32.59, 23.38, 21.68, 18.42, 11.20; minor isomer, 168.56 (*C*=N), 148.11 (*C*-N), 127.07 (C_{Ar}-CH_3), 124.88, 123.17, 55.30, 51.18, 45.46, 32.59, 23.38, 21.68, 18.26, 11.20. Anal. Calcd for $C_{26}H_{32}N_2$: C, 83.82; H, 8.66; N, 7.52. Found: C, 83.70; H, 8.74; N, 7.46.

*Synthesis of 2,6-(^{i}Pr)$_2$C$_6$H$_3$N=C(Ph)C(Ph)=N-2,6-(^{i}Pr)$_2$C$_6$H$_3$ (**L2a**).* Following the above procedure, **L2a** was isolated as orange crystals in 53.7% yield. ^{1}H NMR (300 MHz, $CDCl_3$; δ (ppm) (an isomer ratio of 2.5:1)): major isomer, 7.95−7.00 (m, 16H, Ar-*H*), 2.92 (m, 4H, $CH(CH_3)_2$), 1.08 (d, 24H, $CH(CH_3)_2$); minor isomer, 7.95−7.00 (m, 16H, Ar-*H*), 3.10 (m, 4H, $CH(CH_3)_2$), 0.94 (d, 24H, $CH(CH_3)_2$). ^{13}C NMR (75 MHz, $CDCl_3$; δ (ppm)): major isomer, 166.36 (*C*=N), 145.51 (*C*-N), 137.2, 134.5, 130.7, 128.7, 125.6, 123.6, 122.1, 29.07 (*CH*), 24.62 (*Me*); minor isomer, 162.57 (*C*=N), 145.17 (*C*-N), 137.6, 135.5, 130.1, 128.2, 125.3, 123.6, 122.1, 28.31 (*CH*), 22.89 (*Me*). Anal. Calcd for $C_{38}H_{44}N_2$: C, 86.31; H, 8.39; N, 5.30. Found: C, 86.33; H, 8.40; N, 5.32.

*Synthesis of 2,6-(Me)$_2$C$_6$H$_3$N=C(Ph)C(Ph)=N-2,6-(Me)$_2$C$_6$H$_3$ (**L2b**).* Following the above procedure, **L2b** was isolated as yellow crystals in 69.2% yield. ^{1}H NMR (300 MHz, $CDCl_3$; δ (ppm) (an isomer ratio of 2.1:1)): major isomer, 7.96−6.51 (m, 16H, Ar-*H*), 1.33 (s, 12H, CH_3); minor isomer, many peaks are obscured by major isomer, observed 7.96−6.51 (m, 16H, Ar-*H*), 1.60 (s, 12H, CH_3). ^{13}C NMR (75 MHz, $CDCl_3$; δ (ppm)): major isomer, 164.92 (*C*=N), 147.03 (*C*-N), 137.73 (*CC*=N), 134.72 (C_{Ar}-CH_3), 129.55, 128.34, 127.74, 127.25, 126.36, 123.04, 18.57 (*Me*); minor isomer, 165.19 (*C*=N), 147.44 (*C*-N), 137.73 (*CC*=N), 134.72 (C_{Ar}-CH_3), 130.68, 128.42, 127.91, 127.33, 126.23, 123.15, 18.85 (*Me*). Anal. Calcd for $C_{30}H_{28}N_2$: C, 86.50; H, 6.78; N, 6.72. Found: C, 86.33; H, 6.79; N, 6.51.

*Synthesis of 2,6-(^{i}Pr)$_2$C$_6$H$_3$N=C(4-F-Ph)C(4-F-Ph)=N-2,6-(^{i}Pr)$_2$C$_6$H$_3$ (**L3a**).* Following the above procedure, **L3a** was isolated as orange crystals in 46.8% yield. ^{1}H NMR (300 MHz, $CDCl_3$; δ (ppm) (an isomer ratio of 1.5:1)): major isomer, 7.91−6.41 (m, 14H, Ar-*H*), 2.84 (m, 4H, $CH(CH_3)_2$), 1.09 (d, 24H, $CH(CH_3)_2$); minor isomer, 7.91−6.41 (m, 14H, Ar-*H*), 3.06 (m, 4H, $CH(CH_3)_2$), 0.97 (d, 24H, $CH(CH_3)_2$). ^{13}C NMR (75 MHz, $CDCl_3$; δ (ppm)): major isomer, 164.90 (*C*-F), 160.98 (*C*=N), 145.04 (*C*-N), 135.14, 131.47, 131.44, 124.30, 115.54, 29.02 (*CH*), 24.00 (*Me*); minor isomer, 161.56 (*C*-F), 160.76 (*C*=N), 145.01(*C*-N), 136.09, 131.44, 123.87, 122.66, 115.27, 28.27 (*CH*), 22.69 (*Me*). Anal. Calcd for $C_{38}H_{42}F_2N_2$: C, 80.82; H, 7.50; N, 4.96. Found: C, 80.41; H, 7.49; N, 5.10.

*Synthesis of 2,6-(^{i}Pr)$_2$C$_6$H$_3$N=C(4-Me-Ph)C(4-Me-Ph)=N-2,6-(^{i}Pr)$_2$C$_6$H$_3$ (**L4a**).* Following the above procedure, **L4a** was isolated as yellow crystals in 63.4% yield. ^{1}H NMR (300 MHz, $CDCl_3$; δ (ppm) (an isomer ratio of 1.5:1)): major isomer, 8.03−6.87 (m, 14H, Ar-*H*), 2.78 (m, 4H, $CH(CH_3)_2$), 1.77 (s, 6H, CH_3), 1.07 (d, 24H, $CH(CH_3)_2$); minor isomer, 8.12−6.82 (m, 14*H*, Ar-*H*), 2.76 (m, 4H, $CH(CH_3)_2$), 1.78 (s, 6H, CH_3), 1.09 (d, 24H, $CH(CH_3)_2$). ^{13}C NMR (75 MHz, $CDCl_3$; δ (ppm)): major isomer, 165.73 (*C*=N), 149.45 (*C*-N), 143.81 (*CC*=N), 130.78 (C_{Ar}-Me), 129.37, 128.51, 127.25, 125.73, 122.66, 28.53, 24.42, 18.69; minor isomer, 165.08 (*C*=N), 148.53 (*C*-N), 141.59 (*CC*=N), 131.65 (C_{Ar}-Me), 129.23, 127.96, 127.83, 125.31, 122.78, 27.42, 24.30, 18.47. Anal. Calcd for $C_{40}H_{48}N_2$: C, 86.28; H, 8.69; N, 5.03. Found: C, 86.36; H, 8.56; N, 5.25.

Synthesis of Palladium Complexes. *Synthesis of (2,6-(^{i}Pr)$_2$C$_6$H$_3$N=C(camphyl)C(camphyl)=N-2,6-(^{i}Pr)$_2$C$_6$H$_3$)PdMeCl (**1a**).* To a solution of **L1a** (0.30 g, 0.62 mmol) in dry CH_2Cl_2 (20 mL) was added 0.16 g (0.61 mmol) of (COD)PdMeCl. After the mixture was stirred for 12 h at room temperature, the solution was filtered through Celite, and the solvent of the filtrate was evaporated to give a yellow residue. The residue was washed with 3 × 10 mL hexane and dried under vacuum. The product was isolated as a yellow solid in 41% yield. In $CDCl_3$, trans and cis geometrical isomers were observed in a 2.5:1 ratio on the basis of integration. ^{1}H NMR (300 MHz, $CDCl_3$; δ (ppm)): major isomer, 7.22−7.13 (6H, m, Ar-*H*), 3.18−2.09 (m, 4H, $CH(CH_3)_2$), 1.56−1.37 (m, 5H, camphyl-*H*), 1.36−1.28 (24H, m, $CH(CH_3)_2$), 1.16 (3H, s, camphyl-CH_3), 0.91 (3H, s, camphyl-CH_3), 0.58 (s, 3H, Pd-CH_3); minor isomer, 7.22−7.13 (6H, m, Ar-*H*), 2.97−2.91 (m, 4H, $CH(CH_3)_2$), 1.56−1.37 (m, 5H, camphyl-*H*), 1.36−1.28(24H, m, $CH(CH_3)_2$), 1.16 (3H, s, camphyl-CH_3), 0.62 (3H, s, camphyl-CH_3), 0.53 (s, 3H, Pd-CH_3). ^{13}C NMR (75 MHz, $CDCl_3$; δ (ppm)): major isomer, 184.20, 178.70, 140.53, 140.08, 139.53, 138.96, 138.65, 137.87, 128.00, 127.14, 124.30, 123.78, 123.21, 58.07, 51.82, 31.77, 29.16, 28.4, 25.60, 24.88, 24.43, 23.03, 18.10, 11.6, 2.32; minor isomer, 183.31, 177.78, 140.21, 139.98, 139.37, 138.84, 138.54, 127.82, 126.87, 123.93, 123.56, 122.92, 57.04, 50.67, 31.23, 28.67, 28.4, 25.36, 24.66, 24.16, 21.98, 11.61, 4.27. Anal. Calcd for $C_{34}H_{48}N_2$PdMeCl: C, 65.51; H, 8.01; N, 4.37. Found: C, 65.34; H, 7.89; N, 4.32.

*Synthesis of (2,6-(CH$_3$)$_2$C$_6$H$_3$N=C(camphyl)C(camphyl)=N-2,6-(CH$_3$)$_2$C$_6$H$_3$)PdMeCl (**1b**).* Following the above procedure, **1b** was isolated in 83% yield. In $CDCl_3$, trans and cis geometrical isomers were observed in a 1.5:1 ratio on the basis of integration. ^{1}H NMR (300 MHz, $CDCl_3$; δ (ppm)): major isomer, 7.10−6.99 (6H, m, Ar-*H*), 2.37−2.28 (12H, q, Ar-CH_3), 2.01−1.51 (5H, m, camphyl-*H*), 1.15 (3H, s, camphyl-CH_3), 0.87 (3H, s, camphyl-CH_3), 0.56 (3H, d, camphyl-CH_3), 0.46 (3H, d, Pd-CH_3); minor isomer, 7.10−6.99 (6H, m, Ar-*H*), 2.37−2.28 (12H, q, Ar-CH_3), 2.01−1.51 (5H, m, camphyl-*H*), 1.15 (3H, s, camphyl-CH_3), 0.87 (3H, s, camphyl-CH_3), 0.51 (3H, d, camphyl-CH_3), 0.38 (3H, d, Pd-CH_3). ^{13}C NMR (75 MHz, $CDCl_3$; δ (ppm)): major isomer, 184.61, 179.03, 143.34, 142.48, 129.47, 128.75, 128.42, 127.63, 127.18, 126.03, 57.81, 51.89, 32.08, 23.30, 19.59, 19.00, 18.56, 17.82, 10.92, 0.18; minor isomer, 183.85, 178.14, 142.59, 141.98, 129.24, 128.57, 128,13, 127.50, 127.00, 126.26, 56.62, 50.60, 31.53, 22.77, 19.14, 18.73, 17.82, 10.74, 1.95. Anal. Calcd for $C_{26}H_{32}N_2$PdMeCl: C, 61.25; H, 6.66; N, 5.29. Found: C, 60.93; H, 6.54; N, 5.31.

*Synthesis of (2,6-(i-Pr)$_2$C$_6$H$_3$N=C(Ph)C(Ph)=N-2,6-(i-Pr)$_2$C$_6$H$_3$)-PdMeCl (**2a**).* Following the above procedure, **2a** was isolated in 32% yield. ^{1}H NMR (300 MHz, $CDCl_3$; δ (ppm)): 7.01−7.04, 6.77−6.98 (m, 16H, Ar-*H*), 3.12−3.24 (m, 4H, $CH(CH_3)_2$), 0.94−0.96 (d, 12H, $CH(CH_3)_2$), 0.72 (s, 3H, Pd-CH_3). ^{13}C NMR (75 MHz, $CDCl_3$; δ (ppm)): 174.15, 169.73, 142.05, 138.75, 138.17, 133.54, 133.32, 130.15, 129.03, 128.91, 128.04, 124.06, 123.29, 29.54, 29.09, 23.43, 23.15, 6.06. Anal. Calcd for $C_{38}H_{44}N_2$PdMeCl: C, 68.31; H, 6.91; N, 4.09. Found: C, 68.08; H, 6.83; N, 3.83.

*Synthesis of (2,6-(CH$_3$)$_2$C$_6$H$_3$N=C(Ph)C(Ph)=N-2,6-(CH$_3$)$_2$C$_6$H$_3$)-PdMeCl (**2b**).* Following the above procedure, **2b** was isolated in 92% yield. ^{1}H NMR (300 MHz, $CDCl_3$; δ (ppm)): 6.76−6.70 (m, 6H, Ar-*H*), 6.79−6.97 (m, 10H, Ar-*H*), 2.33−2.34 (d, 12H, Ar−CH_3), 0.61 (s, 3H, Pd−CH_3). ^{13}C NMR (75 MHz, $CDCl_3$; δ (ppm)): 174.4, 169.6, 144.42, 133.54, 133.32, 130.34, 128.80, 127.99, 127.37, 126.92, 126.32, 19.33, 18.84, 4.25. Anal. Calcd for $C_{30}H_{28}N_2$PdMeCl: C, 64.93; H, 5.45; N, 4.88. Found: C, 64.95; H, 5.67; N, 4.83.

*Synthesis of (2,6-(i-Pr)$_2$C$_6$H$_3$N=C(4′-F-Ph)C(4′-F-Ph)=N-2,6-(i-Pr)$_2$C$_6$H$_3$)PdMeCl (**3a**).* Following the above procedure, **3a** was isolated in 47% yield. ^{1}H NMR (300 MHz, $CDCl_3$; δ (ppm)): 6.77−6.81, 6.98−7.01, 7.10−7.14 (m, 14H, Ar-*H*), 3.17−3.25 (m, 4H, $CH(CH_3)_2$), 0.94−0.98 (d, 12H, $CH(CH_3)_2$), 0.73 (s, 3H, Pd−CH_3). ^{13}C NMR (75 MHz, $CDCl_3$; δ (ppm)): 172.72, 168.44, 164.57, 161.15, 141.87, 141.77, 138.54, 138.00, 131.40, 128.18, 127.49, 124.07, 115.85, 115.56, 29.49, 29.05, 23.43, 23.14, 6.26. Anal. Calcd for $C_{38}H_{42}F_2N_2$PdMeCl: C, 64.91; H, 6.29; N, 3.88. Found: C, 64.58; H, 6.31; N, 3.85.

dx.doi.org/10.1021/om300380b | *Organometallics* 2012, 31, 6054−6062

Table 3. Crystal Data and Structure Refinement Details for Complexes 2a, 3a, C1a, and $(L2b)_2Pd(BAF)_2$

	2a	3a	C1a	$(L2b)_2Pd(BAF)_2\cdot0.2H_2O\cdot0.33(Et_2O,C_6H_{14})$
empirical formula	$C_{39}H_{47}ClN_2Pd$	$C_{39}H_{45}ClF_2N_2Pd$	$C_{71}H_{69}BF_{24}N_2O_2Pd$	$C_{127.33}H_{88}B_2F_{48}N_4O_{0.53}Pd$
formula wt	685.64	721.62	1555.49	2726.03
cryst syst	monoclinic	monoclinic	monoclinic	triclinic
space group	$P2_1/c$	$P2_1/c$	$P2_1/n$	$P\bar{1}$
a (Å)	21.262(4)	10.0707(10)	28.532(3)	16.721
b (Å)	9.4135(17)	40.419(4)	14.8505(15)	17.548
c (Å)	17.715(3)	18.8682(15)	35.569(4)	24.927
α (deg)	90	90	90	74.65
β (deg)	92.592(3)	111.797(4)	106.844(2)	87.55
γ (deg)	90	90	90	76.33
V (Å^3)	3541.9(11)	7131.2(11)	14 424(3)	6851.9
Z	4	8	8	2
D(calcd) (g/cm^3)	1.286	1.344	1.433	1.321
F(000)	1432	2992	6336	2748
cryst size (mm)	0.20 × 0.15 × 0.10	0.30 × 0.30 × 0.20	0.42 × 0.41 × 0.22	0.43 × 0.24 × 0.22
θ range (deg)	1.92−28.41	1.54−27.08	1.49−27.11	1.30−26.00
index ranges	$-28 \le h \le 15$	$-11 \le h \le 12$	$-35 \le h \le 36$	$-20 \le h \le 20$
	$-9 \le k \le 12$	$-51 \le k \le 51$	$-19 \le k \le 10$	$-21 \le k \le 21$
	$-23 \le l \le 23$	$-21 \le l \le 24$	$-45 \le l \le 45$	$-30 \le l \le 30$
no. of rflns collected/unique (R_{int})	18 864/8545 (0.0476)	41 962/15 461 (0.0326)	85 249/31 620 (0.0766)	51 806/26 407 (0.0620)
data completeness (%)	95.9	98.6	99.2	97.9
no. of data/restraints/params	8545/0/388	15 461/0/649	31 620/85/1915	26 407/215/1825
goodness of fit on F^2	1.038	1.226	1.099	1.100
final R indices ($I > 2\sigma(I)$)	R1 = 0.0587	R1 = 0.0684	R1 = 0.1149	R1 = 0.0984
	wR2 = 0.1393	wR2 = 0.1777	wR2 = 0.3035	wR2 = 0.2778
R indices (all data)	R1 = 0.1154	R1 = 0.0902	R1 = 0.2120	R1 = 0.1726
	wR2 = 0.1673	wR2 = 0.1914	wR2 = 0.3725	wR2 = 0.3422
largest diff peak and hole (e Å^{-3})	1.535, −1.021	2.180, −3.039	6.391, −1.663	2.731, −0.961

*Synthesis of (2,6-(i-Pr)$_2$C$_6$H$_3$N═C(4′-CH$_3$-Ph)C(4′-CH$_3$-Ph)═N-2,6-(i-Pr)$_2$C$_6$H$_3$)PdMeCl (**4a**).* Following the above procedure, **4a** was isolated in 64% yield. ^{1}H NMR (300 MHz, $CDCl_3$; δ (ppm)): 6.66−7.13 (m, 14H, Ar-*H*), 3.12−3.19 (m, 4H, C*H*(CH$_3$)$_2$), 2.46 (d, 6H, C*H*$_3$), 0.91−0.97 (d, 12H, CH(C*H*$_3$)$_2$), 0.67 (s, 3H, Pd-C*H*$_3$). ^{13}C NMR (75 MHz, $CDCl_3$; δ (ppm)): 169.69, 166.37, 145.61, 145.53, 142.32, 140.56, 138.79, 138.19, 135.22, 130.71, 129.10, 128.85, 124.06, 123.88, 123.35, 29.00, 28.93, 24.76, 23.94, 23.88, 5.74. Anal. Calcd for $C_{40}H_{48}N_2PdMeCl$: C, 69.00; H, 7.20; N, 3.92. Found: C, 69.28; H, 7.31; N, 3.87.

General Procedure for the Synthesis of Cationic Palladium Catalysts [(ArN═C(R)C(R)═NAr)Pd(CH$_2$)$_3$C(O)OMe]$^+$BAF$^-$. A glass reactor was used to add 1.1 equiv of MA to a mixture of 1 equiv of NaBAF and 1 equiv of (ArN═C(R)C(R)═NAr)PdMeCl suspended in 25 mL of Et_2O, and the reaction mixture was stirred for 24 h at room temperature. Sodium chloride was removed from the reaction mixture via filtration, yielding a clear orange-yellow solution. The Et_2O was removed under vacuum, and the product was washed with hexane and dried under vacuum.

*[(ArN═C(R)C(R)═NAr)Pd^{II}(CH$_2$)$_3$C(O)OMe]$^+$BAF$^-$ (**C1a**; Ar = 2,6-(i-Pr)$_2$C$_6$H$_3$, R = Camphyl).* **C1a** was synthesized according to the above general procedure using **1a** (140 mg, 0.22 mmol), NaBAF (195 mg, 0.22 mmol), and MA (22 μL). The resulting yellow powder was isolated in 83% yield. ^{1}H NMR (300 MHz, $CDCl_3$; δ (ppm)): 7.18−6.90 (m, 6H, Ar-*H*), 3.50 (s, 3H, OMe), 3.00 (m, 4H, C*H*(CH$_3$)$_2$), 2.61(t, 2H, C*H*$_2$C(O)), 2.14 (m, 1H, tertiary hydrogen on camphor), 1.92 (m, 4H, C*H*$_2$ on camphor), 1.47 (t, 2H, PdC*H*$_2$), 1.34, 1.25, and 1.21 (m, 24H, CH(C*H*$_3$)$_2$), 0.95 (s, 6H, C*H*$_3$ on camphor), 0.73 (s, 3H, C*H*$_3$ on camphor), 0.54 (pentet, 2H, PdCH$_2$C*H*$_2$CH$_2$C(O)). ^{13}C NMR (75 MHz, $CDCl_3$; chemical shift of characteristic peaks; δ (ppm)): 187.90 (C═O), 185.72 (*C*═N); upfield region, 57.31, 54.41, 51.64, 50.85, 35.28, 30.89, 28.95 (*C*H(CH$_3$)$_2$), 23.97 (CH(*C*H$_3$)$_2$), 23.38, 22.51, 21.67, 17.30, 10.67. Anal. Calcd for $C_{71}H_{69}BF_{24}N_2O_2Pd$: C, 54.82; H, 4.47; N, 1.80. Found: C, 54.95; H, 4.46; N, 1.72.

*[(ArN═C(R)C(R)═NAr)Pd^{II}(CH$_2$)$_3$C(O)OMe]$^+$BAF$^-$ (**C1b**; Ar = 2,6-(CH$_3$)$_2$C$_6$H$_3$, R = Camphyl).* **C1b** was synthesized according to the above general procedure using **1b** (288 mg, 0.54 mmol), NaBAF (482 mg, 0.54 mmol), and MA (53.8 μL). The resulting yellow powder was isolated in 80% yield. ^{1}H NMR (300 MHz, $CDCl_3$; δ (ppm)): 7.19−7.04 (m, 6H, Ar-*H*), 2.07 (m, 1H, tertiary hydrogen on camphor), 1.92 (m, 4H, C*H*$_2$ at camphor), 2.42, 2.35, and 2.28 (m, 12H, (Ar-C*H*$_3$)), 0.92 (s, 6H, C*H*$_3$ on camphor), 0.68 (s, 3H, C*H*$_3$ on camphor), 3.49 (s, 3H, OMe), 2.63 (t, 2H, C*H*$_2$C(O)), 1.34(t, 2H, PdC*H*$_2$), 0.54 (pentet, 2H, PdCH$_2$C*H*$_2$CH$_2$C(O)). ^{13}C NMR (75 MHz, $CDCl_3$; chemical shift of characteristic peaks; δ (ppm)): 188.27 (C═O), 183.13 (*C*═N); upfield region, 56.75, 54.32, 52.09, 50.63, 35.50, 31.01, 23.17, 22.66, 22.41, 18.16 (Ar-C*H*$_3$), 17.00, 9.99. Anal. Calcd for $C_{63}H_{53}BF_{24}N_2O_2Pd$: C, 52.43; H, 3.70; N, 1.94. Found: C, 52.09; H, 3.93; N, 1.74.

*[(ArN═C(R)C(R)═NAr)Pd^{II}(CH$_2$)$_3$C(O)OMe]$^+$BAF$^-$ (**C2a**; Ar = 2,6-(i-Pr)$_2$C$_6$H$_3$, R = Ph).* **C2a** was synthesized according to the above general procedure using **2a** (213 mg, 0.31 mmol), NaBAF (275 mg, 0.31 mmol), and MA (30.8 μL). The resulting orange powder was isolated in 30% yield. ^{1}H NMR (300 MHz, $CDCl_3$; δ (ppm)): 7.21−6.79 (m, 16H, Ar-*H*), 2.99 (m, 4H, C*H*(CH$_3$)$_2$), 1.41, 1.34, and 1.26 (m, 24H, CH(C*H*$_3$)$_2$), 3.47 (s, 3H, OMe), 2.63 (t, 2H, C*H*$_2$C(O)), 1.54 (t, 2H, PdC*H*$_2$), 0.66 (pentet, 2H, PdCH$_2$C*H*$_2$CH$_2$C(O)). ^{13}C NMR (75 MHz, $CDCl_3$; chemical shift of characteristic peaks; δ (ppm)): 182.71 (C═O), 177.65 (*C*═N); upfield region, 54.54, 35.29, 32.84, 29.23 (*C*H(CH$_3$)$_2$), 23.69 (CH(*C*H$_3$)$_2$), 22.23. Anal. Calcd for $C_{75}H_{65}BF_{24}N_2O_2Pd$: C, 56.32; H, 4.10; N, 1.75. Found: C, 55.95; H, 4.13; N, 1.57.

*[(ArN═C(R)C(R)═NAr)Pd^{II}(CH$_2$)$_3$C(O)OMe]$^+$BAF$^-$ (**C2b**; Ar = 2,6-(CH$_3$)$_2$C$_6$H$_3$, R = Ph).* **C2b** was synthesized according to the above general procedure using **2b** (226 mg, 0.40 mmol), NaBAF (351 mg, 0.40 mmol), and MA (39.0 μL). The resulting orange powder was isolated in 59% yield. ^{1}H NMR (300 MHz, $CDCl_3$; δ (ppm)): 7.19−6.76 (m, 16H, Ar-*H*), 2.38 and 2.29 (m, 12H, (Ar-C*H*$_3$)), 3.68 (s, 3H, OMe), 2.66 (t, 2H, C*H*$_2$C(O)), 1.44 (t, 2H, PdC*H*$_2$), 0.69 (pentet,

dx.doi.org/10.1021/om300380b | Organometallics 2012, 31, 6054−6062

2H, $PdCH_2CH_2CH_2C(O)$). ^{13}C NMR (75 MHz, $CDCl_3$; chemical shift of characteristic peaks; δ (ppm)): 183.33 (C═O), 178.38 (C═N); upfield region, 53.52, 35.59, 31.32, 23.41, 18.15 (Ar−CH_3). Anal. Calcd for $C_{67}H_{49}BF_{24}N_2O_2Pd$: C, 54.11; H, 3.32; N, 1.88. Found: C, 53.86; H, 3.41; N, 1.69.

[(ArN═C(R)C(R)═NAr)Pd^{II}$(CH_2)_3$C(O)OMe]$^+$BAF$^-$ (**C4a**; *Ar = 2,6-(i-Pr)$_2$C$_6$H$_3$, R = 4-Me-Ph*). **C4a** was synthesized according to the above general procedure using **4a** (296 mg, 0.41 mmol), NaBAF (367 mg, 0.41 mmol), and MA (40.7 μL). The resulting orange powder was isolated in 42% yield. ^1H NMR (300 MHz, $CDCl_3$; δ (ppm)): 7.19−6.73 (m, 14H, Ar-*H*), 2.93 (m, 4H, $CH(CH_3)_2$), 1.86 (s, 6H, CH_3 on phenyl backbone), 1.45−1.29 (m, 24H, $CH(CH_3)_2$), 3.52 (s, 3H, OMe), 2.61 (t, 2H, $CH_2C(O)$), 1.57 (t, 2H, $PdCH_2$), 0.63 (pentet, 2H, $PdCH_2CH_2CH_2C(O)$). ^{13}C NMR (75 MHz, $CDCl_3$; chemical shift of characteristic peaks; δ (ppm)): 183.68 (C═O), 178.41 (C═N); upfield region, 57.86, 36.28, 34.69, 32.84, 29.56 ($CH(CH_3)_2$), 27.99 ($CH(CH_3)_2$), 22.78. Anal. Calcd for $C_{77}H_{69}BF_{24}N_2O_2Pd$: C, 56.82; H, 4.27; N, 1.72. Found: C, 56.63; H, 4.25; N, 1.86.

The NMR data indicate the sole presence of a single isomer, the six-membered chelate. All single crystals of palladium complexes were grown from a mixed dichloromethane or ethyl ether/hexane solution by slow evaporation. Crystal data and structure refinement details for palladium complexes **2a**, **3a**, **C1a**, and (**L2b**)$_2$Pd(BAF)$_2$ are shown in Table 3.

■ ASSOCIATED CONTENT

Ⓢ Supporting Information

CIF files giving detailed crystallographic data of palladium complexes. This material is available free of charge via the Internet at http://pubs.acs.org.

■ AUTHOR INFORMATION

Corresponding Author

*E-mail: gaohy@mail.sysu.edu.cn (H.G.); ceswuq@mail.sysu.edu.cn (Q.W.). Tel: 86-20-84113250. Fax: 86-20-84114033.

Notes

The authors declare no competing financial interest.

■ ACKNOWLEDGMENTS

Financial support by the NSFC (Projects 20974125, 51173209, and 21174164), CNPC Innovation Foundation, and the Fundamental Research Funds for the Central Universities (Project 10lgpy10) are gratefully acknowledged.

■ REFERENCES

(1) Johnson, L. K.; Killian, C. M.; Brookhart, M. *J. Am. Chem. Soc.* **1995**, *117*, 6414.
(2) Johnson, L. K.; Mecking, S.; Brookhart, M. *J. Am. Chem. Soc.* **1996**, *118*, 267.
(3) Mecking, S.; Johnson, L. K.; Wang, L.; Brookhart, M. *J. Am. Chem. Soc.* **1998**, *120*, 888.
(4) Britovsek, G. J. P.; Gibson, V. C.; Wass, D. F. *Angew. Chem., Int. Ed.* **1999**, *38*, 428.
(5) Guan, Z.; Cotts, P. M.; McCord, E. F.; McLain, S. J. *Science* **1999**, *283*, 2059.
(6) Cotts, P. M.; Guan, Z.; McCord, E. F.; McLain, S. J. *Macromolecules* **2000**, *33*, 6945.
(7) Guan, Z. *Chem. Eur. J.* **2002**, *8*, 3086.
(8) Guan, Z. *J. Polym. Sci. A: Polym. Chem.* **2003**, *41*, 3680.
(9) Ittel, S. D.; Johnson, L. K.; Brookhart, M. *Chem. Rev.* **2000**, *100*, 1169.
(10) Mecking, S. *Coord. Chem. Rev.* **2000**, *203*, 325.
(11) Mecking, S. *Angew. Chem., Int. Ed.* **2001**, *40*, 534.
(12) Gobson, V. C.; Spitzmesser, S. K. *Chem. Rev.* **2003**, *103*, 283.
(13) Zhang, J.; Wang, X.; Jin, G.-X. *Coord. Chem. Rev.* **2006**, *250*, 95.
(14) Domski, G. J.; Rose, J. M.; Coates, G. W.; Bolig, A. D.; Brookhart, M. *Prog. Polym. Sci.* **2007**, *32*, 30.
(15) Anselment, T. M. J.; Vagin, S.-I.; Rieger, B. *Dalton Trans.* **2008**, 4537.
(16) Guo, L.; Gao, H.; Li, L.; Wu, Q. *Macromol. Chem. Phys.* **2011**, *212*, 2029.
(17) Guan, Z.; Cotts, P. M. *Polym. Mater. Sci. Eng.* **2001**, *84*, 382.
(18) Ye, Z.; Zhu, S. *Macromolecules* **2003**, *36*, 2194.
(19) Guan, Z.; Popeney, C. S. *Topics in Organometallic Chemistry*; Springer: Berlin, Heidelberg, 2009.
(20) Chen, G.; Ma, X. S.; Guan, Z. *J. Am. Chem. Soc.* **2003**, *125*, 6697.
(21) Chen, G.; Guan, Z. *J. Am. Chem. Soc.* **2004**, *126*, 2662.
(22) Chen, G.; Huynh, D.; Felgner, P. L.; Guan, Z. *J. Am. Chem. Soc.* **2006**, *128*, 4298.
(23) Zhang, K.; Wang, J.; Subramanian, R.; Ye, Z.; Lu, J.; Yu, Q. *Macromol. Rapid Commun.* **2007**, *28*, 2185.
(24) Zhang, K.; Ye, Z.; Subramanian, R. *Macromolecules* **2008**, *41*, 640.
(25) Shi, X.; Zhao, Y.; Gao, H.; Zhang, L.; Zhu, F.; Wu, Q. *Macromol. Rapid Commun.* **2012**, *33*, 374.
(26) Tempel, D. J.; Johnson, L. K.; Huff, R. L.; White, P. S.; Brookhart, M. *J. Am. Chem. Soc.* **2000**, *122*, 6686.
(27) Camacho, D. H.; Salo, E. V.; Guan, Z. *Angew. Chem., Int. Ed.* **2004**, *43*, 1821.
(28) Popeney, C. S.; Camacho, D. H.; Guan, Z. *J. Am. Chem. Soc.* **2007**, *129*, 10062.
(29) Popeney, C. S.; Guan, Z. *Organometallics* **2005**, *24*, 1145.
(30) Popeney, C. S.; Levins, C. M.; Guan, Z. *Organometallics* **2011**, *30*, 2432.
(31) Schleis, T.; Heinemann, J.; Spaniol, T. P.; Mülhaupt, R.; Okuda, J. *Inorg. Chem. Commun.* **1998**, *1*, 431.
(32) Liu, F.; Hu, H.; Xu, Y.; Guo, L.; Zai, S.; Song, K.; Gao, H.; Zhang, L.; Zhu, F.; Wu, Q. *Macromolecules* **2009**, *42*, 7789.
(33) Borkar, S.; Yennawar, H.; Sen, A. *Organometallics* **2007**, *26*, 4711.
(34) Camacho, D. H.; Salo, E. V.; Guan, Z.; Ziller, J. W. *Organometallics* **2005**, *24*, 4933.
(35) Schmid, M.; Eberhardt, R.; Klinga, M.; Leskelä, M.; Rieger, B. *Organometallics* **2001**, *20*, 2321.
(36) Gottfried, A. C.; Brookhart, M. *Macromolecules* **2001**, *34*, 1140.
(37) Azoulay, J. D.; Schneider, Y.; Galland, G. B.; Bazan, G. C. *Chem. Commun.* **2009**, *45*, 6177.
(38) Zai, S.; Liu, F.; Gao, H.; Li, C.; Zhou, G.; Guo, L.; Zhang, L.; Zhu, F.; Wu, Q. *Chem. Commun.* **2010**, *46*, 4321.
(39) Gao, H.; Hu, H.; Zhu, F.; Wu, Q. *Chem. Commun.* **2012**, *48*, 3312.
(40) Zai, S.; Gao, H.; Huang, Z.; Hu, H.; Wu, H.; Wu, Q. *ACS Catal.* **2012**, *2*, 433.